

# The Study on the Vibration and Noise Characteristics Caused by Electromagnetic Force of the Fan Motor with the Offset in the Axial Direction

Masaki Ogushi<sup>1</sup>, Koki Shiohata<sup>2</sup>, Zhong Yan<sup>1</sup>, Atsushi Taroda<sup>1</sup>, Takako Otsuka<sup>1</sup>, Yasuhiro Ikehara<sup>1</sup>, and Yoichi Kawai<sup>1</sup>

<sup>1</sup>Minebea Co., Ltd. Electric Device & Component Manufacturing HQ, Fukuroi-shi, Japan

<sup>2</sup>Ibaraki University, Hitachi-shi, Japan

Email: {mogushi, yanzhong, ataroda, tkfukuda, ikehara, yoichikawai}@minebea.co.jp, koki.shiohata.ayu@vc.ibaraki.ac.jp

**Abstract**—Fan motors are used in many equipments. Common requirements for the fan motors are high efficiency, high air capacity, and low vibration and noise. Recent changes in many people's lifestyle brought up reduction and noise of fan motors as an important issue. In this study, features on the vibration and noise in the axial direction were explained, and resonance frequency between electromagnetic force and structural natural frequency were investigated by numerical simulation. First, equations of motion for the fan motor were expressed. And a 3-D model was build, and electromagnetic forces (in the radial, tangential and axial direction) were calculated. Next, a 3-D model for structural vibration was build, and vibration characteristics were calculated. Finally, resonance phenomena caused by harmonics of the electromagnetic force that occurred in the fan motor in the axial direction were clarified.

**Index Terms**—rotary machinery, fan motor, noise, vibration of mechanism, electromagnetic induced vibration, natural frequency

## I. INTRODUCTION

In the current market of electric motors, more and more importance is placed on low noise and low vibration as well as high power and high efficiency. Since an increase in power density and rotational speed of a motor can cause more noise and vibration, measures must be taken to reduce the noise and vibration. There have been considerable researches on motors with lower vibration and noise in terms of both electromagnetic and structural dynamics.

In the field of research on electromagnetic forces in electric motors studies on the effect of pole-slot combination [1], and modeling of excitation forces caused by harmonic components of the current in a brushless motor [2], have been reported. In the field of electromagnetic analysis on electromagnetic

characteristics of electrical motors, researchers on electromagnetic analysis using the nodal force method [3], and calculation of the characteristics of axial-gap solid motor [4] have been reported. In the field of study of numerical simulation of electromagnetic forces, researches on methods for analyzing vibration and noise induced by electromagnetic force [5], and methods for analyzing electromagnetic force in rotary machines using three-dimensional models [6], have been reported. In the field of study on natural frequency and normal mode, researches on the vibration of stator on the motors using modal analysis method [7] has been reported. Finite element studies have been done on natural frequencies of the stator. [8]

A fan motor is an electrical machine which consists of a motor and a fan, and used in a machinery cooling system. It is used in various kinds of equipments such as electrical household appliances, information equipments, OA equipments, in-vehicle equipments, and industrial equipments. Common requirements for fan motors are high efficiency, high air capacity, and low vibration and noise. Recent changes in many peoples' lifestyle brought up reduction of vibration and noise of fan motors as an important issue.

As for noise and vibration in a fan motor, a number of studies have been done on fluid noise of a fan [9], [10] [11]. However few papers discuss the issue in terms of both electromagnetic and structural vibration. Especially, there are no studies on noise and vibration in the axial direction. A paper [12] reports the study that analyzed mechanisms of vibration and noise generation in a small fan motor experimentally and concluded that significant noise is caused by resonance between harmonics of electromagnetic force in the axial direction and natural frequency of the fan motor.

In this study, the features on the vibration and noise in the axial direction were explained, and resonance phenomenon between electromagnetic force and structural natural frequency were investigated by numerical simulation. First, a 3-D model for

electromagnetic analysis was built, and electromagnetic forces (in the radial, tangential, and axial direction) were calculated. Next, a 3-D model for structural vibration model was built, and vibration characteristics were calculated. Finally, resonance phenomena caused by harmonics of the electromagnetic force that occurred in the fan motor in the axial direction were clarified.

II. VIBRATION AND NOISE CHARACTERISTICS OF THE OPERATING FAN MOTOR

Fig. 1 shows fan the motor model and Table I shows specification. Main results of vibration and noise characteristics obtained by experimental methods were described as follows. Please refer to reference [12] for measuring methods.

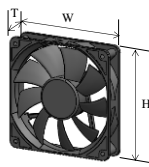
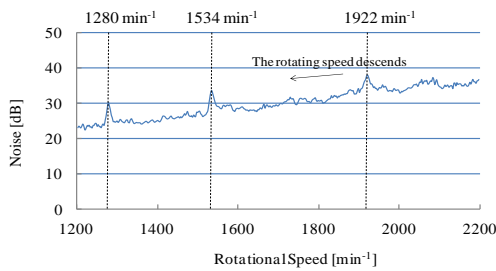


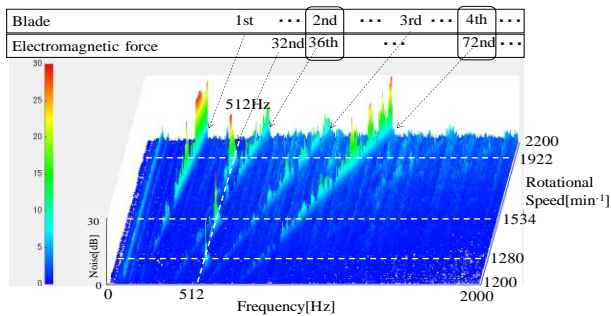
Figure 1. Model of the fan motor

TABLE I. SPECIFICATION OF THE FAN MOTOR

Width: W × Height: H × Thickness: T [mm]	120 × 120 × 25
Number of poles	4
Number of stator slots	4
Number of blades	9
Operating speed [min <sup>-1</sup> ]	2200



(a) Overall noise



(b) 3-D visualization of noise

Figure 2. Noise level

Rotational speed was continuously decreased from 2200 min<sup>-1</sup> to 1200 min<sup>-1</sup> while the measurements were taken. Fig. 2(a) shows the overall noise level. Significant peaks were present at 1922min<sup>-1</sup>, 1534min<sup>-1</sup>, and 1280min<sup>-1</sup>. Fig. 2(b) shows a three-dimensional representation of noise plotted against frequency and

rotational speed that corresponds to the overall noise described in Fig. 2(a). Fig. 3 shows the results of frequency analysis at 1922 min<sup>-1</sup> where the significant peak occurred. In Fig. 3, the rounded squares indicate frequencies of 576 Hz and 1152 Hz where blade-passing frequencies, which are determined by the number of blades, coincided with harmonic frequencies of electromagnetic forces. For this reason, significant peaks were present at 576 Hz and 1152 Hz. Frequency of 512 Hz is both a structural natural frequency of structure and the 32nd harmonics of the electromagnetic force. These facts imply that the significant resonance at 512 Hz was caused by the 32nd component of electromagnetic force at 1922min<sup>-1</sup>.

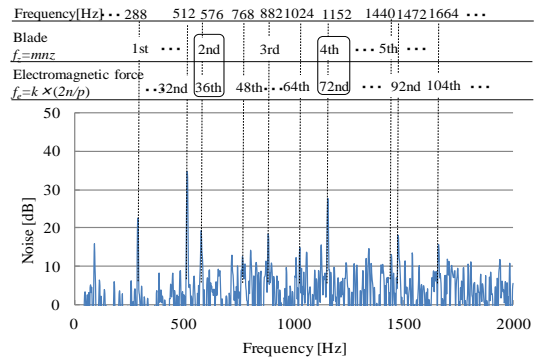


Figure 3. Noise level at 1922 min<sup>-1</sup>

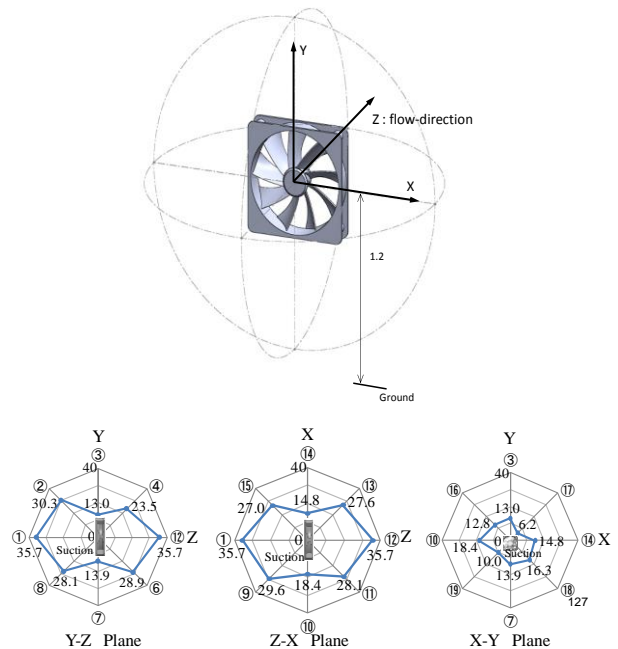
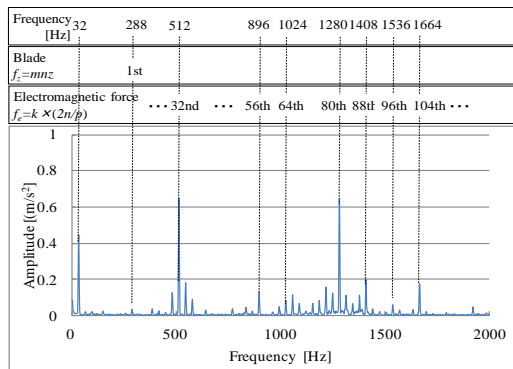


Figure 4. Noise level at 512 Hz measured at multiple microphone position

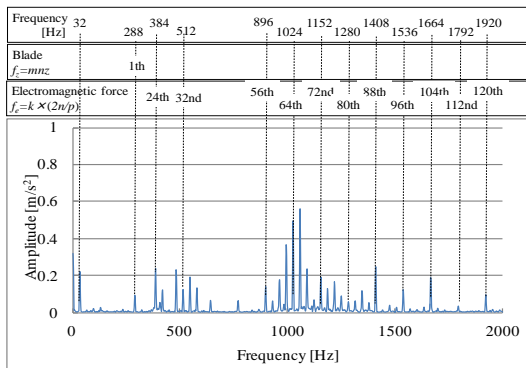
Fig. 4, which describes noise levels measured at multiple microphone position, shows the directivity of noise in each plane. Compared with the noise levels in the X and Y, the noise level in the direction Z was higher by about 20 dB. These facts indicate that the noise at 512 Hz mainly generated in the axial direction.

Fig. 5 shows results of frequency analysis on vibration in the axial direction at 1922 min<sup>-1</sup>. Compared to the

radial direction (Fig. 5(b)), vibration amplitude level at 512 Hz was high in the axial direction (Fig. 5(a)). These results of the analysis on noise and vibration of the operating fan motor indicate that a maximum peak was generated by resonance between the natural frequency for the 0th nodal diameter of the fan (umbrella mode) in which the entire impeller vibrates in the axial direction in the same phase and harmonic component of electromagnetic force.



(a) Axial direction



(b) Radial direction

Figure 5. Vibration amplitude at 1922 min<sup>-1</sup>.

Fig. 6 shows vibration amplitudes of the 32nd electromagnetic force in the axial and radial direction versus rotational speed. Vibration amplitude in the axial direction has a prominent peak at 1922min<sup>-1</sup> when the rotational speed was shifted with a focus on the 32nd electromagnetic harmonic component. On the other hand, vibration amplitude in the radial direction, and no prominent peaks were present.

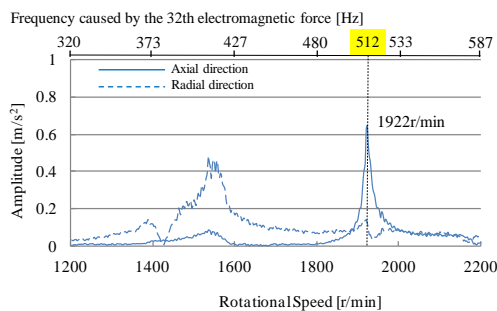


Figure 6. Vibration amplitude of the 32nd electromagnetic force in the axial and radial direction versus rotational speed

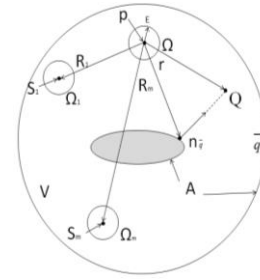


Figure 7. Acoustic analysis model

It was estimated that significant noise peak caused by electromagnetic force were vibration-radiated-noise generated from the blades in the axial direction of the fan. Fig. 7 shows acoustic analysis model. When  $\Phi(p)$  is a velocity potential at arbitrary point  $p$  in a domain  $V$ , the relations between the sound pressure  $P(p)$  and particle velocity  $v_n(\bar{q})$  in the tangential direction at the boundary surface  $A$  is described as follows. [5]

$$P(p) = -j\omega\rho\Phi(p) \quad (1)$$

$$v_n(\bar{q}) = -(\partial\Phi(\bar{q})/\partial n_{\bar{q}}) \quad (2)$$

where  $j$  is the imaginary unit,  $\omega$  is the angular velocity,  $\rho$  is density of medium, and  $n_{\bar{q}}$  is the normal vector at any position  $\bar{q}$  of boundary surface.

### III. ELECTROMAGNETIC ANALYSIS

In this and next chapters, phenomena of vibration and noise of the fan motor caused by electromagnetic force were clarified by numerical simulation. Equation of motion for the fan motor is expressed follows.

$$[M]\{\ddot{x}\} + [C]\{\dot{x}\} + [K]\{x\} = \{f(t)\} \quad (3)$$

where  $[M]$  is the mass matrix,  $[C]$  is the damping matrix, and  $[K]$  is the stiffness matrix. A motor and a fan are included in  $[M]$ ,  $[K]$ ,  $[C]$  matrix, and  $\{f(t)\}$  is the external force matrix. Matrix of  $\{f(t)\}$  is coupled with electromagnetic force, unbalance force, and fluid dynamic force. Fig. 8 shows the procedures for electromagnetic and structural vibration analysis.

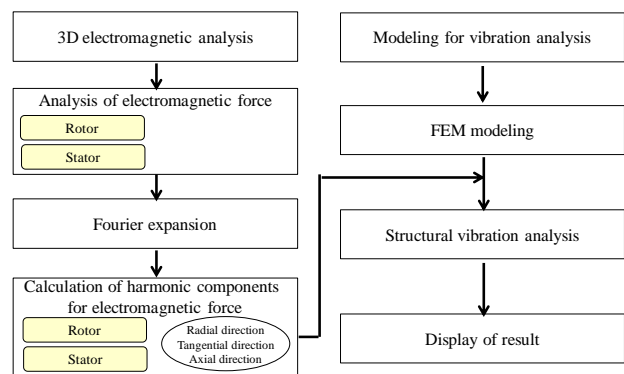


Figure 8. Procedures of electromagnetic and structural vibration analysis

In this chapter, first, electromagnetic force in the radial, tangential, and axial direction were calculated by simulation. Harmonic components were also investigated by Fourier series expansion. Next, the influence of the offset between the magnet and the stator on harmonic components of electromagnetic force was investigated.

A. The Model of Electromagnetic Analysis

As described in chapter 2, noise level (radiated noise) was biggest at 1922min<sup>-1</sup> where resonance between the 32nd harmonic component of the electromagnetic force and the natural frequency of the fan motor occurred. Fig. 9 shows the model of the electromagnetic analysis, which consists of a stator, winding, rotor flame, and magnet. Only one side of rotor flame is which a fan installed was included in the model. Fig. 10 shows spatial relationship of the magnet and rotor in Fig. 9.

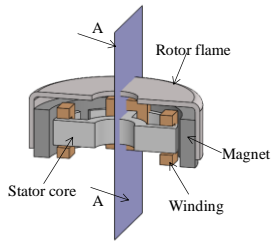


Figure 9. Motor model for electromagnetic analysis

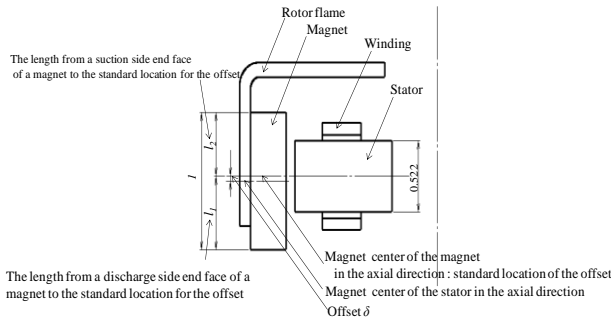


Figure 10. Spatial relationship of the magnet and rotor A-A section in Fig. 8

TABLE II. SPECIFICATION OF THE MOTOR MODEL

Specification	value
Motor winding	Number of turn: 260
	Ratio magnetic permeability: 1
Magnet	Retentivity: bH <sub>c</sub> [Oe]: 2160
	BH <sub>max</sub> [MGOe]: 1.4
	Ratio magnetic permeability: 1.06
The length from a suction side end face of a magnet to the standard location for the offset : a	0.535
The length from a discharge side end face of a magnet to the standard location for the offset : b	0.465
Offset : δ	0.035

Table II shows parameters used in the electromagnetic analysis. This describes dimensionless parameters where the axial length of magnet is 1. In this case, the axial length of the stator is 0.522, and offset δ in the axial direction is 0.035. We used three-dimensional electromagnetic analysis because thinness of the rotor and the stator in the axial direction and the offset between the rotor and the stator in the axial direction were likely to cause electromagnetic force in the axial direction.

The electromagnetic force is mathematically expressed follows.

$$\vec{F} = \sum_i \vec{f}_i \tag{4}$$

$$\vec{f}_i = -(\vec{T} \cdot \nabla N_i) dv \tag{5}$$

where  $\vec{F}$  is electromagnetic force,  $\vec{f}$  is electromagnetic force acting on a node in the FEM model,  $\vec{T}$  is Maxwell stress tensor, and  $N$  is shaped function.

$$\vec{T} = \frac{1}{2\mu} \begin{bmatrix} B_x^2 - B_y^2 - B_z^2 & 2B_x B_y & 2B_x B_z \\ 2B_y B_x & B_y^2 - B_z^2 - B_x^2 & 2B_y B_z \\ 2B_z B_x & 2B_z B_y & B_z^2 - B_x^2 - B_y^2 \end{bmatrix} \tag{6}$$

where μ is ratio magnetic permeability, B<sub>x</sub> B<sub>y</sub> B<sub>z</sub> are magnetic flux density in respective directions.

When the electromagnetic analysis with a constant-voltage source and a constant rotational speed was performed, an electric current wasn't determined, only by circuit constants because induced voltage and inductance affect current. Therefore, transient phenomenon was involved on the first step stage in the analysis of the electromagnetic force. In this study, data from 6 steps and later steps, which did not include transient stages, were used.

B. The Analysis of the Electromagnetic Force

Electromagnetic force which acted on the magnet and the stator were investigated at 1922min<sup>-1</sup> where the noise level was biggest. To investigate the influence of offset between the magnet and the stator has on harmonic components of electromagnetic force, analysis was performed on several cases of offsets (-0.0875, -0.07, -0.035, 0, 0.035, 0.07, 0.0875) in the axial direction.

Fig. 11 shows calculated results of the electromagnetic force in the radial, tangential, and axial direction which acted on the magnet. Maximum value of electromagnetic force was written in Fig. 11. The level of electromagnetic force in the radial direction was highest among three directions. The level of electromagnetic force in the tangential direction was the second highest. Also, the electromagnetic force in the axial direction occurred as well.

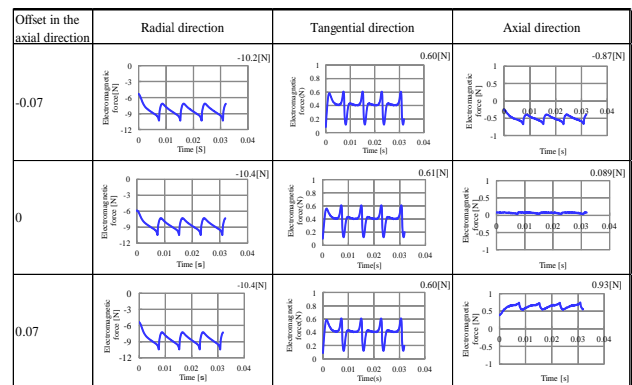


Figure 11. Electromagnetic force in the radial, tangential, and axial direction at 1922 min<sup>-1</sup>

When the offset in the axial direction was changed, the level of electromagnetic force in the radial and tangential direction stayed unchanged. Electromagnetic force was in

the same phase regardless of the changes in the offset. On the other hand, when offset in the axial direction was bigger, the electromagnetic force in the axial direction was also bigger. When the offset value was switched from positive to negative or vice versa, the electromagnetic force was in the opposite phase.

Frequency analysis on electromagnetic force was performed, and harmonic components were investigated. Fig. 12 shows the results of frequency analysis and harmonic components of electromagnetic force in the radial and axial direction at the offset of 0.035. Harmonic components were present in the axial direction as well.

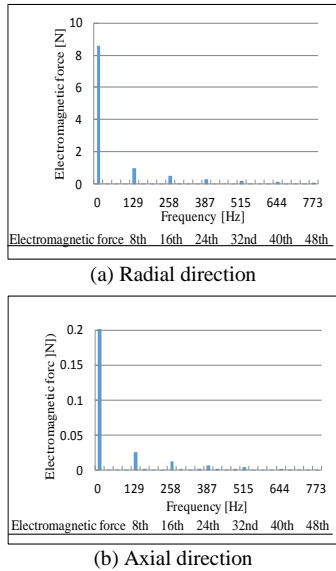


Figure 12. The frequency analysis and harmonic components of electromagnetic force at 1922 min<sup>-1</sup>

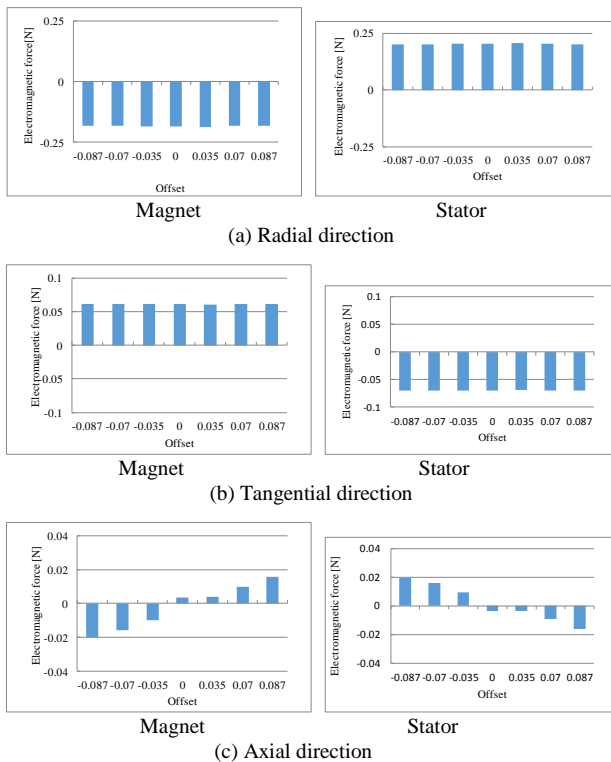


Figure 13. 32nd electromagnetic force at 1922 min<sup>-1</sup>

Fig. 13 shows the relationship between the offset in the axial direction and the 32nd component of electromagnetic force which acted in the magnet and the stator. Fig. 13(a) shows the relation between the offset in the axial direction and the 32nd component radial direction. Fig. 13(b) shows the relation between the offset in the axial direction and the 32nd component in the tangential direction. Fig. 13(c) shows the relation between the offset in the axial direction and the 32nd component in the axial direction.

Even when the offset in the axial direction changed, the level of the 32nd component of electromagnetic force in the radial and tangential direction stayed unchanged. On the other hand, when offset in the axial direction was larger, the 32nd component of electromagnetic force in the axial direction was also greater. When the offset is zero, the 32nd component of electromagnetic force in axial direction was not zero. Since outer rotor structure has a rotor frame only on one side, the harmonic components on electromagnetic force were generated in the axial direction even when the offset was zero.

Fig. 14(a) shows vector representation of magnetic flux vector, and Fig. 14(b) shows magnetic flux lines at 1922min<sup>-1</sup>. The magnet and the stator are hidden in Fig. 14. The flux had components in the axial direction as well as radial and tangential direction, and this is considered to be the cause of harmonic components of the electromagnetic force in the axial direction.

As mentioned above, electromagnetic force had axial components, and that changes in the axial offset made harmonic components of an axial electromagnetic force bigger.

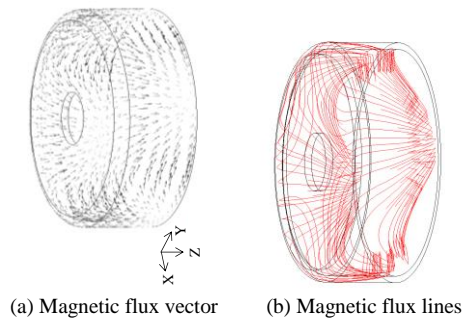


Figure 14. Magnetic flux vector and magnetic flux density at 1922 min<sup>-1</sup>

#### IV. STRUCTURAL VIBRATION ANALYSIS

In this chapter, first, natural frequencies and natural vibration modes were determined by analysis on the structural vibration model with a focus on axial components which had significant peak in actual measurements [12].

Table III shows material properties used in the structural vibration analysis. The number of nodes was 172271, and the number of elements was 88181 in the finite element model. The structural analysis of the fan motor was performed, and main principal vibration modes were investigated. The natural frequency in the axial direction where the noise was biggest was experimentally determined to be 530 Hz [12]. By the

structural analysis, the natural frequency, which corresponds to be experimentally determined natural frequency of 530 Hz, was determined to be 538 Hz. Fig. 15 shows three-dimensional contour figure and a schematic illustration of natural vibration mode at 538 Hz which resulted from the structural analysis. This is vibration mode with the 0th nodal diameter of the fan (umbrella mode) which each blade vibrates in the same phase in the axial direction.

TABLE III. MATERIAL PROPERTIES FOR STRUCTURAL ANALYSIS

Parts	Material	Yong's modulus [Gpa]	Density [Kg/m <sup>3</sup> ]
Blade	Plastic	5.95	1630
Rotor flame	Steel	200	7850
Magnet	Plastic magnet	5	3500
Shaft	Steel	200	7850
Stator	Electromagnetic plate and sheet	200	7850
Casing	Plastic	6.3	1430

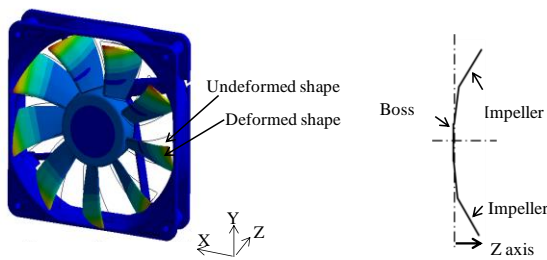


Figure 15. Natural vibration mode at 538 Hz

Therefore, results from both structural vibration analysis and experimental analysis showed the same vibration mode, and the calculation precision was within 2%. As mentioned above, the peak frequency of vibration and noise peak in an operating fan motor was presumed to the natural frequency with the 0th nodal diameter of the fan (umbrella mode).

In chapter 3, when the offset in the axial direction was bigger, the 32th component of electromagnetic force in the axial direction was also bigger. In chapter 4, the peak frequency of vibration and noise in the operating fan motor was presumed to be the natural frequency with the 0th zero nodal diameter of the fan (umbrella mode).

As mentioned above, it was presumed that the noise peak in operating fan motor was caused by resonance between the harmonic component of the electromagnetic force in the axial direction caused by the offset and the natural frequency with the 0th nodal diameter of the fan (umbrella mode).

## V. CONCLUSION

By using three-dimensional magnetic field analysis and structural vibration analysis, following conclusions regarding vibration and noise in a fan motor with an offset in the axial direction were obtained.

(1) The results of the three-dimensional magnetic analysis showed that electromagnetic force had axial components, and that changes in the axial offset made harmonic components of an axial electromagnetic force bigger.

(2) In the structural vibration analysis, the peak frequency of the vibration and noise in an operating fan motor were estimated to the natural frequency with the 0th nodal diameter of the fan (umbrella mode).

(3) Conclusion (1) and (2) lead to another conclusion that the noise peak in an operating fan motor was caused by resonance between the harmonic component of the electromagnetic force in the axial direction caused by the offset and the natural frequency with the 0th nodal diameter of the fan (umbrella mode).

## REFERENCES

- [1] T. Kobayashi, F. Tajima, M. Ito, and S. Shibukawa, "Effect of slot combination on acoustic noise from induction motor," *IEEE Transaction on Magnetics*, vol. 33, no. 2, pp. 2032-2035, 1993.
- [2] D. Verdyck, R. Eimans, and W. Gwysen, "An approach to modeling of magnetically an exited forces in electrical machines," *IEEE Transaction on Magnetics*, vol. 29, no. 2, pp. 2032-2035, 1993.
- [3] A. Kameari, "Electromagnetic force calculation by nodal force method," *IEEJ*, pp. 95-104, 1993 (in Japanese).
- [4] M. Valtonen, A. Palviainen, and J. Pyrhonen, "Electromagnetic field of 3D structure of axial-flux solid-rotor induction motor," in *Proc. SPEEDOM*, 2006, pp. s39-12- s39-16.
- [5] K. Shiohata, *et al.*, "A method for analyzing electromagnetic-force-induced vibration and noise analysis," *IEEJ*, vol. 118, no. 11, pp. 1301-1302, 1998 (in Japanese).
- [6] T. Talahashi, T. Nakata, M. Nakano, and H. Morishige, "Analysis and measurement of 3-D model of verification of electromagnetic force calculation," *IEEJ*, pp. 29-37, 1993 (in Japanese).
- [7] D. Verdyck and R. Belmans, "An acoustic model for a permanent magnet machine: Modal shapes and magnetic forces," *IEEE Transaction on Industry Applications*, vol. 30, no. 6, pp. 1625-1631, 1994.
- [8] K. Itomi, S. Noda, I. Suzuki, and F. Ishibashi, "Analysis for natural frequency of stator core in induction motor," *Transaction of the Japan Society of Mechanical Engineering, Series C*, vol. 64, no. 624, pp. 2833-2839, 1998 (in Japanese).
- [9] T. Zhu and T. Carolus, "Experimental and numerical investigation of tip clearance noise of an axial fan using a lattice Boltzman method," in *Proc. International Conference on Fan Noise, Technology and Numerical Method*, France, 2015.
- [10] M. Sturm and T. Carolus, "Tonal noise of an isolated axial fan rotor due to inhomogeneous coherent flow structures at the intake," in *Proc. International Conference on Fan Noise, Technology and Numerical Method*, France, 2012.
- [11] S. Kadota, K. Kawaguchi, M. Suzuki, K. Matsui, and K. Kikuyama, "Experimental study on low-noise multiblade fan (1<sup>st</sup> report, visualization of three-dimentional flow between blades)," *Transaction of the Japan Society of Mechanical Engineering Society C*, vol. 60, no. 570, pp. 102-107, 1994 (in Japanese).
- [12] M. Ogushi, K. Shiohata, T. Otsuka, and Z. Yan, "Noise and vibration analysis on a fan motor," *ISEF2013*, ID#130, 2013.



**Masaki Ogushi** was born in Japan in 1953. He received his Bachelor's in Engineering from Kobe University, Kobe, Hyogo, Prefecture, and his Dr. in Engineering from Ibaraki University, Mito, Ibaraki Prefecture in 2015. He had worked for Panasonic Corporation (Matsushita Electric Industrial Co., Ltd.) from 1977 to 2009. He has been working for Minebea Co., Ltd. from 2009. Dr. Ogushi is currently an engineer at Minebea Co., Ltd. He is also a member of JSME, IEEJ and Turbomachinery Society of Japan.



Dr. Shiohata is currently fellow and honorary member of JSME, and member of Turbomachinery Society of Japan.

**Koki Shiohata** was born in Japan in 1947. He received his Bachelor's degree in Engineering from Ibaraki University, Mito, Ibaraki Prefecture, Japan, in 1970, and his Master's degree in Engineering from Ibaraki University in 1972. He received his Doctor's degree in Engineering from Tokyo Institute Technology in 1985. He had worked for Hitachi, Ltd. from 1972 to 2000. He had worked as Professor for Ibaraki University from 2000 to 2013. He has been working as professor emeritus for Ibaraki University from 2013.



**Takako Otsuka** was born in Japan in 1984. She received her Bachelor's degree in Engineering from Shizuoka University, Hamamatsu, Shizuoka Prefecture, Japan, in 2007. She has been working for Minebea Co., Ltd. from 2007. She is currently an engineer at Minebea Co., Ltd. She is also a member of JSME, and Turbomachinery Society of Japan.



**Yan Zhong** was born in China in 1980. She received her Bachelor's degree in Computer and Information Science from Aichi Prefectural University, Nagakute, Aichi Prefecture, Japan, in 2008. She had worked for MapQuest Corporation from 2008 to 2010. She has been working for Minebea Co., Ltd. from 2010. She is currently an engineer at Minebea Co., Ltd.



**Yasuhiro Ikehara** was born in Sendai, Japan in 1985. He received his Bachelor's degree in Mechanical Engineering from Tohoku University, Sendai, Miyagi Prefecture, Japan in 2010, and his Master's degree in Mechanical Engineering from Tohoku University, Sendai, Miyagi, Prefecture, Japan in 2012. He has been working for Minebea Co., Ltd. since 2012 as an engineer.



**Atsushi Taroda** was born in Japan in 1983. He received his Bachelor's degree in Engineering from Tokai University, Hiratsuka, Kanagawa Prefecture, Japan, in 2006. He has been working for Minebea Co., Ltd. from 2006. He is currently an engineer at Minebea Co., Ltd.



**Yoichi Kawai** was born in Japan in 1964. He received his Bachelor's degree in Engineering from Yamanashi University, Kofu, Yamanashi Prefecture, Japan, in 1987. He had worked for National Micro Motor Co., Ltd. from 1987 to 2004. He has been working for Minebea Co., Ltd. from 2004. He is currently an engineer at Minebea Co., Ltd.